

## Mass Spectrometric Study of Carbon Cluster Formation in Laser Ablation of Graphite at 355 nm

Young-Mi Koo, Young-Ku Choi, Kee Hag Lee, and Kwang-Woo Jung\*

Department of Chemistry, Wonkwang University, Iksan 570-749, Korea

Received October 10, 2001

The ablation dynamics and cluster formation of  $C_n^+$  ions ejected from 355 nm laser ablation of a graphite target in vacuum are investigated using a reflectron time-of-flight (TOF) mass spectrometer. At low laser fluence, odd-numbered cluster ions with  $3 \leq n \leq 15$  are predominantly produced. Increasing the laser fluence shifts the maximum size distribution towards small cluster ions, implying the fragmentation of larger clusters within the hot plume. The temporal evolution of  $C_n^+$  ions was measured by varying the delay time of the ion extraction pulse with respect to the laser irradiation, providing significant information on the characteristics of the ablated plume. Above a laser fluence of  $0.2 \text{ J/cm}^2$ , large cluster ions ( $n \geq 30$ ) are produced at relatively long delay times, indicating that atoms or small carbon clusters aggregate during plume propagation. The dependence of the intensity of ablated  $C_n^+$  ions on delay time after laser irradiation shows that the most probable velocity of each cluster ion decreases with cluster size.

**Keywords :** Graphite, Clusters, Laser ablation, Time-of-flight mass spectrometry.

### Introduction

The laser ablation of graphite has attracted attention because of its utility in the fabrication of thin films of newly discovered materials such as fullerenes,<sup>1</sup> single-walled nanotubes,<sup>2</sup> and diamond-like carbon (DLC).<sup>3</sup> Carbon clusters are particularly interesting because they display fascinating structural and spectroscopic properties, are important in astrophysical processes, and play a significant role in combustion and soot formation. Carbon clusters have been found to grow through the aggregation of the species vaporized from graphite.<sup>1,4</sup> An alternative pathway of carbon cluster formation was suggested by Bloomfield *et al.*<sup>5</sup> and Cox *et al.*,<sup>6</sup> who proposed that carbon clusters form via fragmentation of initially formed larger clusters and laser-desorbed carbon dust. This proposal is supported by recent studies by Achiba *et al.*<sup>7,8</sup> on the mass distribution of neutral carbon clusters generated by laser vaporization of graphite in He, which found that carbon clusters formed through the fragmentation of large hot clusters into smaller clusters. In spite of the extensive investigation into carbon clusters over the past decade, many aspects of these systems are still to be unraveled, not only in the understanding of the chemical and physical properties of carbon clusters but also in clarifying the mechanism of cluster formation.

The temporal velocity profile of ejected materials is an important characteristic in the production of reactive species and for determining the structural quality of the deposited film, because the kinetic energy of the species is a key controlling parameter.<sup>9,10</sup> Although laser-ablated plasmas have been studied to some extent, the dynamics of the interaction between laser light and materials, as well as the detailed

aspects of laser-induced plume formation and expansion, are not fully understood. This is particularly the case for carbon clusters formed at UV wavelengths. Study of the spatial and velocity distribution of the ablated species during the initial stage of ejection and expansion enhances our knowledge of ablation dynamics.

This paper presents a study of the mass distribution of positive carbon-cluster ions produced by laser ablation of graphite at 355 nm. The laser-induced plume from a graphite target under high vacuum conditions is characterized by measuring TOF mass spectra with varying laser fluence. The dependence of the observed  $C_n^+$  signals on the laser fluence is discussed on the basis of the energetics of cluster formation and fragmentation. The time-dependent flow dynamics of plume expansion are also investigated by time-delayed extraction of ions ablated off-axis to the flight direction of the mass spectrometer. The results provide direct evidence that small clusters aggregate during plume expansion to form higher cluster ions.

### Experimental Section

A schematic diagram of the experimental setup is shown in Figure 1. Laser ablation of a graphite target was carried out in a vacuum chamber (base pressure  $< 2 \times 10^{-7}$  Torr) combined with a reflectron TOF mass spectrometer. A target rod (8 mm in diameter) of graphite (99.95% purity, Goodfellow Metal Ltd.) was placed between the ion optics of the extraction region and rotated at 10 rpm to get a fresh target surface after each laser shot. The target location relative to the center of the ion extraction region was fixed at  $h = 1.0$  cm. The third harmonic output (355 nm) of a Q-switched Nd:YAG laser (10 ns pulse width), operated at a repetition rate of 10 Hz, was used to strike the solid target. The radiation was focused by a 40 cm focal length lens to a spot

\*Corresponding author. Fax: +82-63-841-4893; e-mail: kvjung@wonmms.wonkwang.ac.kr

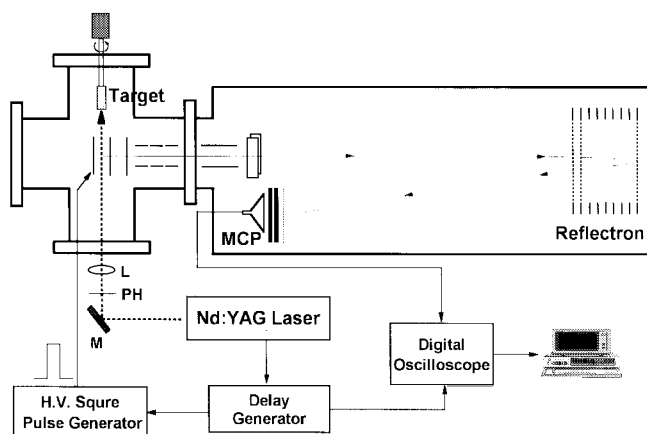


**Figure 1.** Schematic diagram of the experimental setup for pulsed-field/reflectron time-of-flight mass spectrometry. L, lens; PH, pinhole; M, mirror.

size of  $5 \times 10^{-4} \text{ cm}^2$ . The laser fluence at the target surface was varied over the range  $0.06\text{--}0.84 \text{ J/cm}^2$ .

When the ablated plume reached the extraction region of the TOFMS, the positive ions were extracted (typically following a delay of  $\tau_d = 0.3\text{--}2.0 \mu\text{s}$  after the laser shot) by a  $+1700 \text{ V}$  pulsed electric field (Directed Energy, Inc., GRX-3.0K-H), applied to the first grid. The ion extraction pulse has a rise time of  $40 \text{ ns}$  and duration of  $1 \mu\text{s}$ . In this geometry, the ion flight path is at right angles to the velocity vector of the ejected plume. This feature allows us to examine the temporal profile of each ion, permitting accurate measurement of the velocity distribution and the drift velocity of the ionic species. The ions accelerated by the second accelerating grid ( $1.4 \text{ kV}$ ) travel through a  $1 \text{ m}$  long field-free region, which terminates at a double stage reflectron (R. M. Jordan Co.) located at the end of the flight tube. Following the reflectron, the ions travel an additional  $0.64 \text{ m}$  back to a microchannel plate (MCP) detector. In the present experiments the TOF mass spectra were averaged over 2000 laser shots using a  $500\text{-MHz}$  digital oscilloscope (LeCroy 9350A).

## Results and Discussion

Figure 2 shows the TOF mass spectra of carbon cluster ions obtained from  $355 \text{ nm}$  laser irradiation of a graphite target at four different laser fluences. The delay time between the laser shot and the ion extraction pulse was set at  $\tau_d = 800 \text{ ns}$ . At the low laser fluence of  $0.06 \text{ J/cm}^2$ , the spectrum consists mainly of  $\text{C}_n^+$  ions with  $n = 3\text{--}11$  whose yield decreases almost monotonically with increasing cluster size. At a fluence of  $0.12 \text{ J/cm}^2$  the major clusters are  $\text{C}_n^+$  ions with  $n = 3, 5, 7, 11,$  and  $15$  and the ion intensities increase with increasing the fluence up to a value of approximately  $0.4 \text{ J/cm}^2$ . The preferential formation of odd-numbered cluster ions has been previously found in the mass spectra of carbon clusters generated by  $\lambda = 266, 355,$  and  $532 \text{ nm}$  laser vaporization.<sup>11–13</sup> Eyler, *et al.* measured the ionization potentials (IPs) of carbon clusters on the basis of the charge-transfer

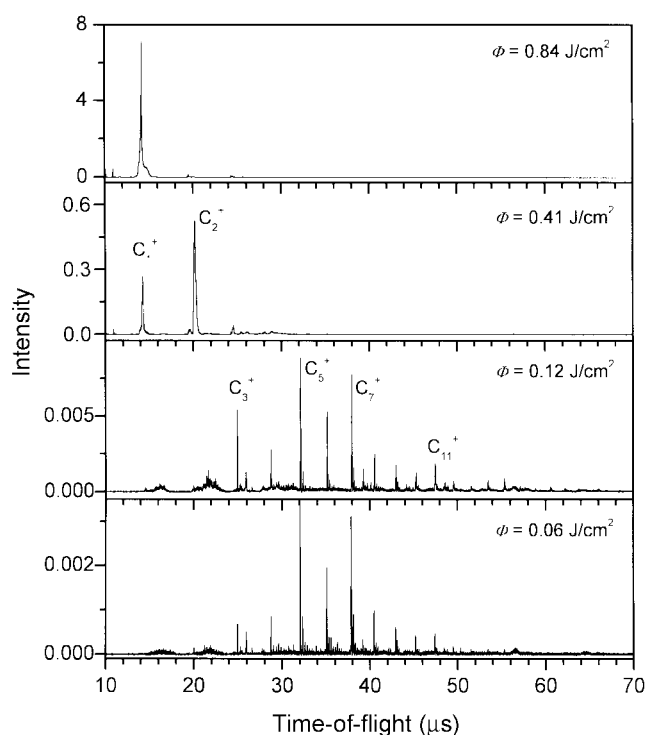


**Figure 2.** TOF mass spectra of laser ablated  $\text{C}_n^+$  ions as a function of laser fluence ( $\tau_d = 800 \text{ ns}$ ).

technique.<sup>14,15</sup> They found that odd-numbered carbon clusters represent minima in a plot of IP over the cluster size. The unusual abundance of these cluster ions may therefore be due to their low IPs rather than to a special degree of stability. However, the relatively low dissociation energies of even-numbered cluster ions also cause the  $n$ -odd species to be more stable than the  $n$ -even species for  $n = 1\text{--}15$ .<sup>16</sup>

When the laser fluence is increased to  $0.41 \text{ J/cm}^2$ , the cluster distribution is shifted to lower mass, with  $\text{C}^+$  and  $\text{C}_2^+$  ions predominating. Above  $0.5 \text{ J/cm}^2$ , only  $\text{C}^+$  is produced. A similar tendency has also been found in a recent study on the laser ablation of graphite at  $266 \text{ nm}$ ,<sup>17</sup> in which  $\text{C}^+$  and  $\text{C}_3^+$  ions became the dominant species as the laser fluence was increased. This result is consistent with the view that the concentration of small cluster ions increases with laser fluence because larger clusters undergo fragmentation within the hot plume. The broad temporal distribution of each cluster peak at high fluence, as compared with the results at low fluence, supports the conjecture that the cluster ions have high kinetic energy due to ion-ion repulsion in the plume at higher ion densities. Therefore, the dependence of the intensity of  $\text{C}_n^+$  ions on laser fluence observed in the present experiments leads us to conclude that at low laser fluence the ablated  $\text{C}_n^+$  ions are formed directly from the graphite surface, whereas at higher fluences the fragmentation of large clusters has a significant contribution. In our experiments we have no direct method of determining whether the fragment ions result from neutral fragmentation followed by ionization or from direct fragmentation of parent ions as a result of absorption of excess laser photons. However, the

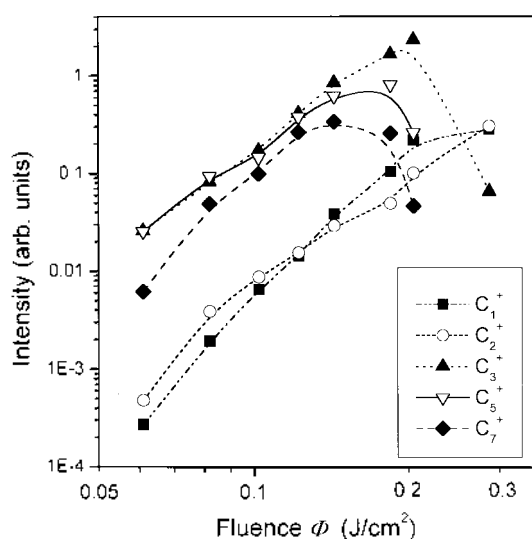


**Figure 3.** Laser-fluence dependence of  $C_n^+$  ions ( $n = 1, 2, 3, 5,$  and  $7$ ) at  $\tau_d = 500$  ns.

fact that direct ionization dominates at low fluence and fragmentation dominates at high fluence suggests that dissociation occurs after the formation of the parent ions.

To shed more light on the ion formation mechanism we investigated the general trends in the ion abundance distribution of the mass spectra as a function of the laser fluence.  $\Phi$  Figure 3 shows the log-log plots of  $C_n^+$  ions ( $n = 1, 2, 3, 5,$  and  $7$ ). The ion signal of each species was obtained by integration of the corresponding TOF spectrum at  $\tau_d = 500$  ns. The intensities of the  $C^+$  and  $C_2^+$  ions increase substantially with laser fluence, whereas those of the  $C_3^+$ ,  $C_5^+$ , and  $C_7^+$  ions exhibit maxima in the region of  $0.15\text{--}0.2$   $J/cm^2$ . The falling off in the slope at higher laser fluence for  $C_3^+$ ,  $C_5^+$ , and  $C_7^+$  provides evidence of saturation. It is also noted that the laser fluence corresponding to the maximum intensity decreases with increasing cluster size. This propensity is in reasonable agreement with the binding (or dissociation) energy of  $C_n^+$  ions, which gradually decreases with cluster size.<sup>18</sup> The saturation-type behavior and subsequent signal decrease in the ion yield data clearly indicate that these ions undergo fragmentation into smaller cluster ions. By increasing the laser fluence, the internal energy of the resulting clusters increases and finally attains the dissociation limit. When the laser fluence exceeds the dissociation limit of the primary  $C_n^+$  ions produced from the target surface, these primary ions dissociate to smaller ions. In such a case, the bond breaking and/or energy release to the translation of fragments should act as a major cooling process for hot particles. Collision-induced dissociation of  $C_n^+$  species with high internal energy may lead to the generation of  $C^+$  and  $C_2^+$ .

To investigate the temporal evolution of the ablated plume we measured the TOF ion signal as a function of the delay time between the laser shot and the repelling electric field applied to the ion optics. The delay time was stepped to reveal the distribution of the ionic species over time. Different traces therefore refer to different slices of the ablation

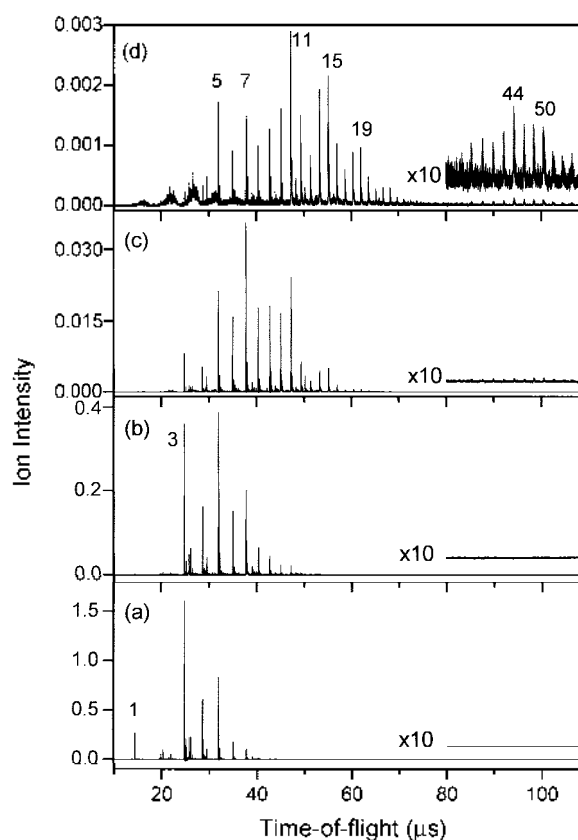


**Figure 4.** TOF mass spectra of laser ablated  $C_n^+$  ions at various delay times  $\tau_d$  between the laser shot and the ion extraction pulse: (a) 300 ns; (b) 500 ns; (c) 700 ns; (d) 900 ns. The laser fluence is  $0.20$   $J/cm^2$ .

plume as it expands in the vacuum. This method offers an excellent means of investigating the time-dependent cluster distribution of the ionic species during the initial stage of plume expansion. The TOF mass spectra of laser ablated  $C_n^+$  ions were plotted as a function of the delay time, as shown in Figure 4. These spectra were obtained using a laser pulse energy of  $0.20$   $J/cm^2$ . The signal intensity of  $C_n^+$  ions drops sharply with delay time  $\tau_d$ . This decrease primarily originates from the spreading of the ablated plume over the space above the target surface during the delay time after laser irradiation. The mass spectrum at  $\tau_d = 300$  ns consists only of small cluster ions ( $1 \leq n \leq 9$ ), whereas increasing the delay time shifts the intensity distribution toward large clusters. This means that the carbon cluster cations are distributed over a wide range of arrival time distributions according to their masses: the small cluster ions travel at a higher velocity whereas the larger cluster ions travel at a lower velocity. This difference in velocity is presumably due to the velocity slip in the supersonic expansion, because larger clusters acquire a lower velocity if they are not involved in sufficient collisions, as will be described in more detail later.

It is intriguing that at the longer delay time of  $\tau_d = 700$  ns heavy cluster ions ( $n \geq 30$ ) appear for arrival times of  $80\text{--}90$   $\mu s$ . These ions are formed only when the laser fluence energy is greater than  $0.2$   $J/cm^2$ , where the fragmentation

into small cluster gives a significant contribution. Upon laser ablation of graphite, a low laser fluence causes mainly desorption and decomposition of large hot particles emitted from the laser-irradiated surface of graphite. In such a cluster formation process, cation formation is mostly accomplished by electron impact ionization by the free electrons escaping from the expanding plasma of the laser ablation. On the other hand, higher fluence promotes further atomization of the targets, resulting in preferential formation of smaller carbon clusters. The resulting small carbon fragments aggregate during plume propagation<sup>19</sup> forming a smooth mass distribution, as shown in Figures 4c and 4d. Alternatively, there exists another cooling channel for the hot particles that might be important in the stabilization of particles emitted from the hot surface. The internal temperature of the ablated large particles would be sufficient to promote spontaneous thermal ionization. As a result, so called "thermionic emission" occurs, producing cations as well as slow electrons. Efficient thermionic ionization may take place in large carbon clusters, which would explain the even-numbered high-mass carbon clusters often observed in the mass spectra.

At  $\tau_d = 900$  ns, two groups of clusters are clearly observed. In the low mass ( $n \leq 30$ ) region of 10–80  $\mu\text{s}$ , odd-numbered clusters show an enhanced intensity, consistent with previous reports.<sup>13,20</sup> In the high mass region ( $n \geq 30$ ), however, only even-numbered clusters including abundant  $\text{C}_{44}^+$  and  $\text{C}_{50}^+$  appear, as has been widely known so far. The observation of large cluster ions at long delay times is readily explained as follows. The laser ablation of graphite at high fluence yields atoms or small clusters via direct evaporation of graphite or intense fragmentation of large carbon particles. The resulting small fragments aggregate to form larger clusters during plume propagation. In the case where few collisions occur, the faster moving carbon species exit the target surface, whereas the slower moving clusters take longer to exit the surface and are therefore more likely to aggregate and grow. We can conclude that collisions caused during the expansion of the vapor from the target surface are responsible for the presence of these clusters, and that gas-phase condensation probably dominates over direct ejection.

In the present experiment, an increase in the delay time between the laser shot and ion extraction pulse corresponds to an increase in the flight time of the collected ions through the axis perpendicular to the TOFMS detection axis. Fast particles appear at shorter delays in these experiments. One of the great strengths of the pulsed-field TOFMS technique is the ability to obtain the temporal profile of each ion by varying the delay time, permitting accurate measurement of the velocity distribution and drift velocity of the ionic species. Figure 5a shows the intensity of cluster ions ablated at a laser fluence of  $0.06 \text{ J/cm}^2$  as a function of delay time of the ion extraction pulse. The  $\text{C}_9^+$  and  $\text{C}_{11}^+$  ion intensities are multiplied by 15 for display purposes. The relatively low intensity of the  $\text{C}^+$  ion precluded estimation of its temporal distribution. The TOF arrival data of each cluster ion show a Maxwell-Boltzmann distribution. In fact, collisions among the evaporated particles in the early stages of plume expansion

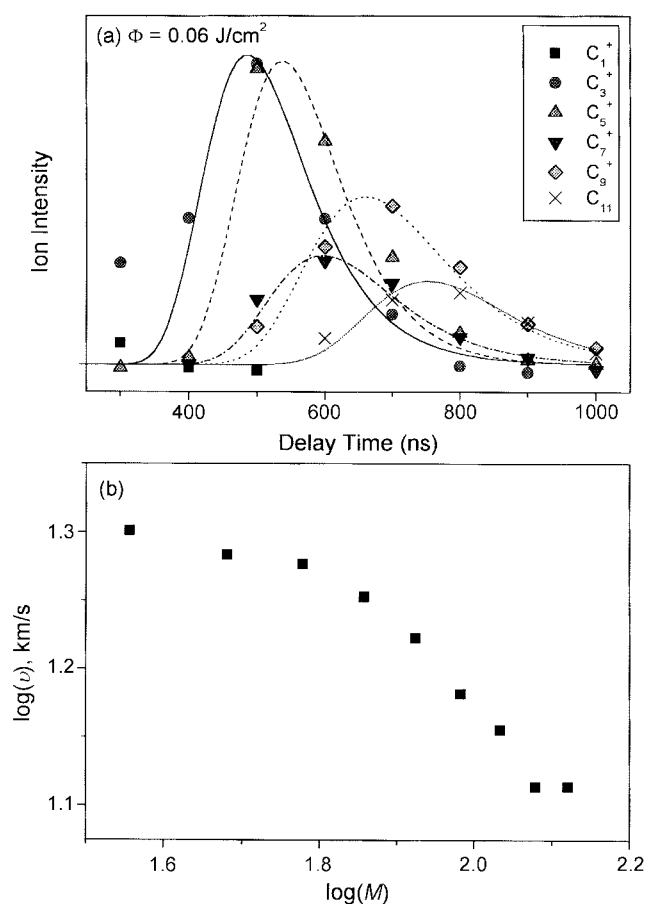


**Figure 5.** (a) Ion intensities of the ablated species as a function of delay time between the laser shot and the ion extraction pulse following  $0.06 \text{ J/cm}^2$  laser irradiation of a graphite target. The  $\text{C}_9^+$  and  $\text{C}_{11}^+$  ion intensities are multiplied by 15 to facilitate comparison. (b) The dependence of cluster ion velocity on cluster mass  $M$ .

in vacuum cause the laser ablation from the solid surface to behave like a nozzle source, creating a strongly forward-peaked particle flux with a large center-of-mass velocity  $v$  along the normal to the target surface. The width of the temporal distributions becomes narrow with increasing laser fluence. The results also support the conjecture that frequent multi-body collisions among the higher-density species ejected from the graphite effectively induce cooling.

The temporal distribution of the ion intensity shows that in general heavier species exhibit a local maximum at longer delay times. The observation of large cluster ions at long delay times implies that these ions have low flow velocities. It is known that the velocity and acceleration of the species in the plume depend on the molecular weight of the species. Since the plume from the graphite target is composed of a range of clusters, the expansion velocities of these species are not the same. The most probable velocities  $v_p$  of  $\text{C}_3^+$ ,  $\text{C}_5^+$ ,  $\text{C}_7^+$ ,  $\text{C}_9^+$ , and  $\text{C}_{11}^+$  ions, calculated from the delay time showing maximum intensity for each species and the distance between the target surface and the ion extraction region, are 20.2, 18.9, 16.7, 14.3, and 13.0 km/s. Their corresponding translational energies ( $E_t$ ) are 74, 111, 121, 114, and 116 eV.

respectively. The high translational energy of the ablated ions is comparable to the values recently estimated by Lade *et al.* (126 eV)<sup>21</sup> and Puzos *et al.* (94.6 eV)<sup>22</sup> from time-gated CCD imaging of C<sup>+</sup> emission resulting from ArF laser ablation of graphite in vacuum.

The high velocity of the ions ejected after laser irradiation could result from the hydrodynamic effect of the plume formed above the target surface. The initial expansion over the time interval of the laser pulse is isothermal. After the laser pulse terminates, the plasma expands adiabatically in the vacuum and the thermal energy of the plasma is converted into kinetic energy. The plasma rapidly cools and the stream velocity begins to increase. Although this effect increases the particle velocities, it is insufficient to account for the high translational energies observed in the present study. The results of the present study can, however, be interpreted in terms of contemporary models of UV laser ablation. In these models the laser pulse induces localized surface excitation and rapid heating, leading to photo- and thermionic electron emission, closely followed by ejection of positive ions. These ions are accelerated out of the local volume as a result of Coulombic attraction (by the expanding electron cloud) and repulsion (by other ions). The large acceleration force of the electric field, generated inside the plume by the difference in velocity between electrons and ions, could contribute to the high velocities of these ions.

Figure 5b shows a plot of the most probable velocity of a cluster ion as a function of its mass  $M$ . The dependence of the ion velocity on  $M$ , determined from the slope of the  $\log v$  versus  $\log M$  plot, was found to be  $-0.36$ . The dependence of the ion drift velocity on cluster mass is weaker than the inverse square root, in agreement with the experimental data of Zheng *et al.*<sup>23</sup> and Sankur *et al.*<sup>24</sup> who reported similar results in studies of the laser ablation of YBCO and Zr<sub>2</sub>O targets, respectively. According to the theoretical predictions for the laser-plasma solid interaction, the maximum velocity of a species should depend on the inverse square root of its molecular weight.<sup>25</sup> Although the measured experimental velocities show the general trend of lower asymptotic velocities for higher masses, the observed dependence is weaker than expected. This discrepancy between theory and experiment is probably due to the interaction (mixing effect) of different atomic species present in the plume. If the particle density is high enough, the collision-induced exchange of momentum that takes place between the ablated species during the initial stages of plume expansion causes all particles to expand with approximately with the same velocity. As the plume expands, the density drops and the expansion approaches a collisionless process. During this regime, the individual particles are free to accelerate and reach their asymptotic velocities. Thus, although the small clusters possess higher expansion velocities, the dependence of the expansion velocities of interacting plume species is less than the predicted inverse square-root dependence. An alternative interpretation is that the large cluster ions with sufficient internal energy spontaneously fragment into lighter ions even at this low laser fluence. In such a case, the expansion

velocities of the small cluster ions produced by fragmentation would be slower than the velocities of small ions produced by primary ablation, resulting in a deviation from the theoretical prediction.

## Conclusion

Laser ablation of a graphite target at 355 nm was investigated using a reflectron TOF mass spectrometer. At low fluence values the mass spectra show peaks characteristic of the odd-numbered C<sub>*n*</sub><sup>-</sup> ions with  $n = 3-15$ . Increasing the laser fluence shifts the cluster distribution to the low mass region, indicating fragmentation of large clusters within the hot plume. As the delay time between the laser shot and the ion extraction pulse is increased, however, large cluster ions with  $n \geq 30$  form due to aggregation of atoms or small clusters as they collide during the expansion of the vapor from the target surface. The time resolved observation of C<sub>*n*</sub><sup>-</sup> ions in a laser-ablated plume presented here also characterizes the axial expansion of the plume, *i.e.*, strictly along a direction perpendicular to the target surface. The compositional variation in the plume arises from the different expansion velocities of species with different cluster masses. Although theory predicts that the ion velocities should vary with the inverse square root of the mass of the species, we observed a weaker dependence, probably because of transfer of momentum in the plasma between different species during the initial stage of the expansion.

**Acknowledgment.** We dedicate this paper to Professor Kyung-Hoon Jung with admiration and gratitude for his scientific creativity, vision, and leadership in research and teaching. This work was supported by grant No. R01-2000-00040 from the Basic Research Program of the Korea Science & Engineering Foundation.

## References

1. Kroto, H. W.; Heath, R. J.; Brien, S. C.; Curl, R. F.; Smalley, R. E. *Nature* **1985**, *318*, 162.
2. Iijima, S.; Ichihashi, T. *Nature* **1993**, *363*, 603.
3. Lowndes, D. H.; Geohagan, D. B.; Puzos, A. A.; Norton, D. P.; Rouleau, C. M. *Science* **1996**, *273*, 898.
4. Smalley, R. E. *Acc. Chem. Res.* **1992**, *25*, 98.
5. Bloomfield, L. A.; Geusic, M. E.; Freeman, R. R.; Brown, W. L. *Chem. Phys. Lett.* **1985**, *121*, 33.
6. Cox, D. M.; Reichmann, K. C.; Kaldor, A. *J. Chem. Phys.* **1988**, *88*, 1588.
7. Kaizu, K.; Kohno, M.; Suzuki, S.; Shiromaru, H.; Moriwaki, T.; Achiba, Y. *J. Chem. Phys.* **1997**, *106*, 9954.
8. Moriwaki, T.; Kobayashi, K.; Osaka, M.; Ohara, M.; Shiromaru, H.; Achiba, Y. *J. Chem. Phys.* **1997**, *107*, 8927.
9. Im, H.-S.; Kim, S.-H.; Choi, Y.-K.; Lee, K. H.; Jung, K.-W. *Bull. Korean Chem. Soc.* **1997**, *18*, 56.
10. Choi, Y.-K.; Im, H.-S.; Jung, K.-W. *Bull. Korean Chem. Soc.* **1998**, *19*, 830.
11. Rohlfsing, E. A.; Cox, D. M.; Kaldor, A. *J. Chem. Phys.* **1984**, *81*, 3322.
12. Gaumet, J. J.; Wakisaka, A.; Shimizu, Y.; Tamori, Y. *J. Chem. Soc. Faraday Trans.* **1993**, *89*, 1667.
13. Choi, Y.-K.; Im, H.-S.; Jung, K.-W. *Int. J. Mass Spectrom.* **1999**, *189*, 115.

14. Ramanathan, R.; Zimmerman, J. A.; Eyer, J. R. *J. Chem. Phys.* **1993**, *98*, 7838.
  15. Bach, S. B.; Eyer, J. R. *J. Chem. Phys.* **1989**, *92*, 358.
  16. Sowa-Resat, M. B.; Hintz, P. A.; Anderson, S. L. *J. Phys. Chem.* **1995**, *99*, 10736.
  17. Kokai, F.; Koka, Y. *Nucl. Instrum. & Methods B* **1997**, *121*, 387.
  18. Raghavachari, K.; Binkley, J. S. *J. Chem. Phys.* **1987**, *87*, 2191.
  19. Kohno, M.; Suzuki, S.; Shiromaru, H.; Moriwaki, T.; Achibe, Y. *Chem. Phys. Lett.* **1998**, *282*, 330.
  20. Choi, Y.-K.; Im, H.-S.; Jung, K.-W. *Bull. Korean Chem. Soc.* **1999**, *20*, 1501.
  21. Lade, R. J.; Ashfold, M. N. R. *Surf. Coat. Technol.* **1999**, *120-121*, 313.
  22. Poretzky, A. A.; Geohegan, D. B.; Jellison, G. E. Jr.; McGibbon, M. M. *Appl. Surf. Sci.* **1996**, *96*, 859.
  23. Zheng, J. P.; Huang, Z. Q.; Shaw, D. T.; Kwok, H. S. *Appl. Phys. Lett.* **1989**, *54*, 280.
  24. Sankur, H.; Denatale, J.; Guming, W.; Nelson, J. G. *J. Vac. Sci. Technol. A* **1987**, *235*, 2869.
  25. Sing, R.; Narayan, J. *Phys. Rev B* **1990**, *41*, 8843.
-